

Structural anisotropy of magnetically aligned single wall carbon nanotube films

B. W. Smith, Z. Benes, D. E. Luzzi, and J. E. Fischer^{a)}

*Department of Materials Science and Engineering and Laboratory for Research on the Structure of Matter,
University of Pennsylvania, Philadelphia, Pennsylvania 19104*

D. A. Walters, M. J. Casavant, J. Schmidt, and R. E. Smalley

Center for Nanoscale Science and Technology, Rice University, Houston, Texas 77259

(Received 21 April 2000; accepted for publication 5 June 2000)

Thick films of aligned single wall carbon nanotubes and ropes have been produced by filtration/deposition from suspension in strong magnetic fields. We measured mosaic distributions of rope orientations in the film plane, for samples of different thicknesses. For an $\sim 1\ \mu\text{m}$ film the full width at half maximum (FWHM) derived from electron diffraction is $25^\circ\text{--}28^\circ$. The FWHM of a thicker film ($\sim 7\ \mu\text{m}$) measured by x-ray diffraction is slightly broader, $35\pm 3^\circ$. Aligned films are denser than ordinary filter-deposited ones, and much denser than as-grown material. Optimization of the process is expected to yield smaller FWHMs and higher densities. © 2000 American Institute of Physics. [S0003-6951(00)05131-7]

Macroscopic oriented arrays of single wall carbon nanotubes (SWNT) would offer many advantages compared to the random tangles of bundled tubes typically found in bulk samples,¹ the ultimate goal being a large single crystal of close-packed tubes. Tangles of small crystallites, or "ropes," consisting of a few to hundreds of tubes, form naturally during SWNT synthesis.² Walters *et al.* have recently succeeded in aligning $\sim 100\text{ mg}$ quantities of SWNT using a strong magnetic field.³ Polarized transmission spectra show that tubes and ropes in suspension adopt a preferred orientation with axes parallel to the field. Thick films, referred to as "buckypaper,"⁴ are achieved by deposition from suspension on to a nylon filter membrane. Ropes in ordinary buckypaper lie preferentially in the plane of the film (see below), while addition of the magnetic field during filter deposition introduces a preferred direction in the plane, as found in scanning electron microscope (SEM) images.³ In this and the following letter, we report quantitative measurements of the structural and transport anisotropies obtained from the initial products of this process.

Two samples were studied, both produced at the National High Magnetic Field Laboratory in a 25 T dc resistive solenoid. The first was prepared using a 25 mm diameter syringe filter in which suspended tubes deposit under axial flow on to a filter membrane normal to the syringe axis. An effective thickness of $\sim 1.3\ \mu\text{m}$ was deduced from the mass/area and an assumed density of 1.33 g/cm^3 for a van der Waals crystal of 1.4 nm diameter tubes. A second, larger and thicker sample was deposited on a cylindrical filter 33 mm diameter and 140 mm long with an active area $\sim 130\text{ cm}^2$. Nanotube orientation with respect to the filter surface is the same as above, but the flow direction is radially outward through the cylindrical filter membrane. With this second technique, we obtained a total mass of 110 mg and a physical thickness of $7\ \mu\text{m}$ by direct measurement and SEM imaging,

yielding a density of 1.21 g/cm^3 . This decreased to 0.89 g/cm^3 after vacuum annealing (see below), indicating that $\sim 30\%$ of the aligned nanotube material is empty volume, a much smaller percentage than is typically found in unaligned buckypaper ($\sim 70\%\text{--}90\%$) or in compacts of as-grown material ($\sim 95\%$).

Structural analysis of the thin sample was carried out using selected area electron diffraction (SAD). Strips of nanotube material $\sim 5\text{ mm}$ long were peeled off the filter⁵ and clamped in a folding transmission electron microscope (TEM) grid. The image in Fig. 1 shows prominent texture corresponding to many aligned ropes. The fraction of grossly misaligned ropes appears to be small, although many which run against the grain are readily apparent. Fewer catalyst particles are found compared to unaligned material, as a result of purification using magnetic field gradients before deposition of the aligned film. Figure 1 also shows that the nanotube bundles are in general not perfectly straight, such that anisotropic diffraction will measure the combined effects of imperfect rope-to-rope alignment and bending/curvature of individual ropes.

SAD fiber diagrams averaged over many ropes ($1\ \mu\text{m}$ aperture) were recorded on film and digitized for analysis, before and after an 11 h 800°C anneal in the microscope (temperature limited by the Cu grid). The upper panel of Fig. 2 shows radial cuts along the equatorial axis (scattering vector $Q \perp$ magnetic field direction H) representing the ordered packing of tubes in a rope. The differential profiles were produced by subtracting the diffuse background at 90° to the rope peaks ($Q \parallel H$; polar axis) from the scattering data through the centroids of the rope peaks (equatorial axis). Shifts in apparent peak positions with annealing are attributed either to grain growth^{6,7} or desorption/deintercalation of surfactant and/or acid residues.⁸ The unannealed profile is typical of acid-purified material.⁴ The sharp leading edge of both profiles is a consequence of the rising background at low Q approaching saturation of the electron microscope film and the nonlinear sigmoidal response curve of photo-

^{a)}Electronic mail: fischer@sol1.lrsm.upenn.edu

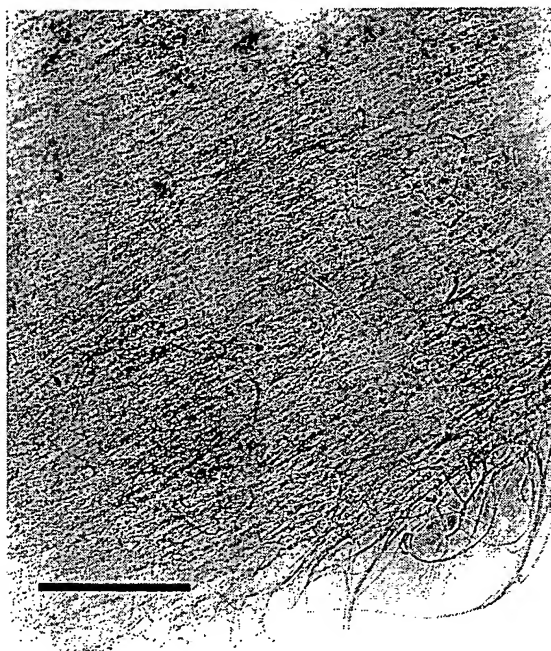


FIG. 1. TEM image of a magnetically aligned SWNT film, showing an area near the torn sample edge. The linear texture, running from the lower left to upper right of the image, is attributed to aligned ropes lying on average parallel to the applied magnetic field (scale bar $0.5\ \mu\text{m}$).

graphic film. Thus, the intensity of the first peak is reduced relative to the higher Q peaks, but the peak positions are reliable.

Mosaic distributions were obtained by summing over the first radial peak (range indicated by the heavy bar) at 21 azimuthal angles centered about the equator. These are plotted in the lower image of Fig. 2 (symbols) along with Gaussian fits (solid curves). The fitted full widths at half maximum (FWHM) are 28.4 ± 1.3 and $25.0 \pm 0.8^\circ$ before and after annealing, respectively. The difference is barely significant. The SAD fiber diagrams also revealed arcs of intensity centered about the polar axis ($Q \parallel H$), with radial Q 's corresponding to the (1,0) and (1,1) in-plane reflections of two-dimensional graphene. The radial and azimuthal intensity distributions of these intratube peaks are consistent with a system of partially aligned ropes, each comprised of a random distribution of tube chiralities.⁹

The second sample was too thick for electron diffraction. The top image of Fig. 3 shows wide-angle x-ray (WAXS) powder profiles^{2,4} of a six-layer sandwich (total thickness $\sim 40\ \mu\text{m}$), measured in reflection before and after 1200°C . Before annealing, the profile is dominated by diffuse small-angle scattering associated with porosity; attempts to measure a mosaic distribution of the very weak Bragg peaks were fruitless. Crystallinity improves dramatically after annealing;⁴ now the profile is consistent with triangular lattice crystallites of $1.3\text{--}1.4\ \text{nm}$ diameter tubes with $0.32\ \text{nm}$ (van der Waals) separation.^{2,4,6,7} Fiber diagrams were measured using small-angle x-ray scattering (SAXS) in transmission with Cu x rays, pinhole optics, a $200\ \mu\text{m}$ beam, helium flight path, and two-dimensional detector. Instrumental background was carefully measured and subtracted from measured profiles prior to further treatment. Mosaic distributions were constructed by integrating 1 degree slices of all the

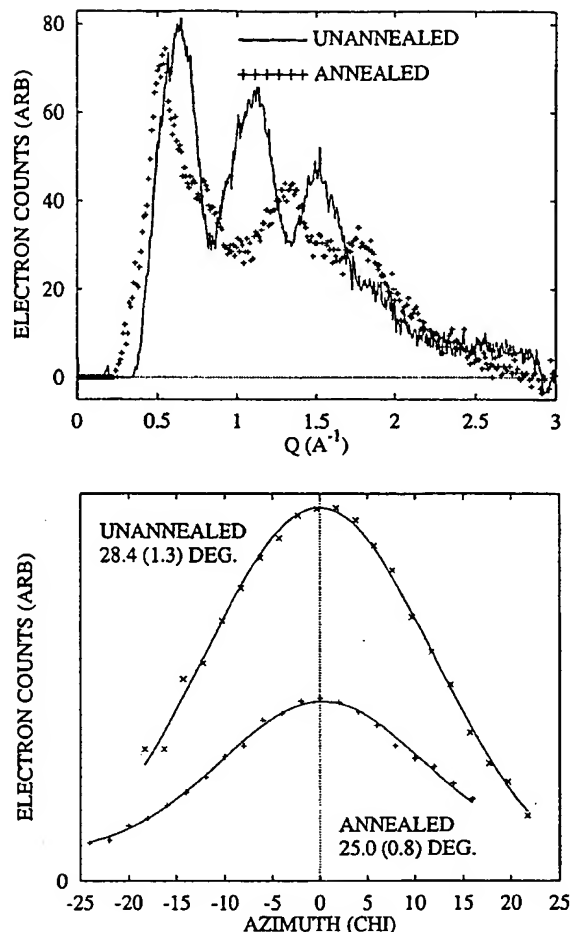


FIG. 2. Top: Equatorial intensity profiles ($Q \perp H$) from electron diffraction recorded before and after *in situ* annealing of the thin H -aligned film at 800°C . These are equivalent to powder profiles of the 2D triangular rope lattice since many ropes are sampled. The Q scale was calibrated using a polycrystalline gold standard. Bottom: mosaic distributions derived from radial slices $\pm 21^\circ$ about the equator (symbols) along with Gaussian fits (solid curves). Radial intensities were summed over the first diffraction maximum at each χ .

counts in the interval $5.6^\circ\text{--}6.6^\circ$ which covers the (1,0) SWNT lattice peak. The results were fitted with Gaussians and are plotted in Fig. 3 (bottom image). The six-film sandwich gave a FWHM of $35^\circ \pm 3^\circ$ (top curve), significantly greater than the 28° thin film result. The middle and lower curves show similar results for two films and a single film. The signal-to-noise ratio gets worse but the FWHM does not change significantly, so we can rule out film-to-film misalignment as a contributing factor to the larger FWHM. While it is tempting to attribute the apparent thickness dependence on a progressive loss of registry, we believe it has more to do with different flow/deposition rates, geometries of the filter support and housing, and/or differences in suspension concentrations. More systematic studies are in progress.

It is interesting to consider the evolution of tube/rope alignment in *three* dimensions, and possible correlations between alignment and density, as we go from as-grown material to filter-deposited buckypaper to the aligned "superbuckypaper" described in this letter. Imagine a Cartesian coordinate system embedded in the sample. In as-grown ma-

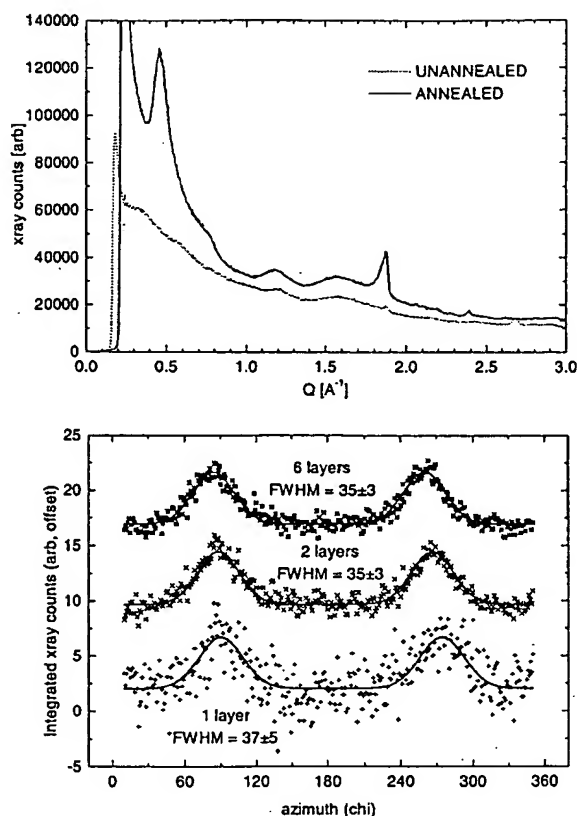


FIG. 3. Top: wide angle x-ray powder profiles from a sandwich of six thick *H*-aligned SWNT films, before and after annealing at 1200 °C. Bottom: mosaic distributions from radial slices of SAXS fiber diagrams of 1, 2, and 6 films (symbols) along with Gaussian fits (solid curves), as shown in Fig. 2.

terial, the tube/rope axes are randomly oriented with respect to all three coordinates, and the apparent density (mass/total volume) is only a few mg/cm³. Filter deposition forces the tube axes to lie preferentially in the film plane (call it the *xy* plane), implying flow-induced partial alignment about two of the three Cartesian axes, namely *x* and *y*. The mosaics describing this hydrodynamic effect should be the same in the *yz* and *xz* planes, respectively, and are expected to depend strongly on the suspension and flow parameters noted above. One measurement of the FWHM characterizing this distribution in ordinary buckypaper is 56°. ¹⁰ The important point is that partial alignment about two axes should produce a large density increase with respect to no alignment, and indeed we have measured buckypaper densities as high as 0.1 g/cm³. Finally, introducing a preferred direction for tube axes in the *xy* plane of the film with a magnetic field, i.e., restricting

tube/rope rotations about the final axis *z*, again increases the density but less dramatically, to the measured value ~0.9 g/cm³. Note that the magnetic field should also reduce the *yz* and *xz* mosaics, and that the *xy* mosaics reported here are no doubt the combined effect of magnetic and hydrodynamic alignment.

The degree of alignment achieved in these first magnetically oriented samples is encouraging. The prospect of large quantities of highly aligned SWNT material should be of interest for realizing the excellent intrinsic mechanical properties in monolithic components, as templates for continuous seeded growth, for controlling the porosity of energy storage media (hydrogen, Li batteries), and as a vehicle for fundamental studies of intertube interactions. The following letter describes the corresponding transport properties. ¹¹

This work was supported by NSF Contract No. DMR98-02560 (electron diffraction; B.W.S. and D.E.L.); the U.S. Department of Energy Contract No. DEFG02-98ER45701 (x-ray diffraction; Z.B., J.E.F); and NASA Award No. NCC 9-77, ONR Grant No. N00014-99-1-0246 and the Welch Foundation (synthesis; D.W., M.C., J.S., R.E.S.). A portion of this work was performed at the National High Magnetic Field Laboratory, which is supported by NSF Cooperative Agreement No. DMR-9527035 and the State of Florida. The authors gratefully acknowledge experimental assistance from L. Qiao and K. Winey.

¹ <http://cnst.rice.edu/tubes/sem.html>

² A. Thess, R. Lee, P. Nikolaev, H. Dai, P. Petit, J. Robert, C. Xu, H. Lee, S. G. Kim, D. T. Colbert, G. Scuseria, D. Tomaneck, J. E. Fischer, and R. E. Smalley, *Science* 273, 483 (1996).

³ D. A. Walters, M. J. Casavant, X. C. Qin, C. B. Huffman, P. J. Boul, L. M. Ericson, E. H. Haroz, M. J. O'Connell, K. Smith, D. T. Colbert, and R. E. Smalley (unpublished).

⁴ A. G. Rinzler, J. Liu, P. Nikolaev, C. B. Huffman, F. J. Rodriguez-Macias, P. J. Boul, A. H. Lu, D. Heymann, D. T. Colbert, R. S. Lee, J. E. Fischer, A. M. Rao, P. C. Eklund, and R. E. Smalley, *Appl. Phys. A: Mater. Sci. Process.* 67, 29 (1998).

⁵ The peeling is strongly anisotropic, *prima facie* evidence for preferred orientation in the film plane.

⁶ J. E. Fischer, A. Claye, and R. S. Lee, *Mol. Cryst. Liq. Cryst. Sci. Technol., Sect. A* 340, 737 (2000).

⁷ S. Rols, R. Almairac, L. Henrard, E. Anglaret, and J.-L. Sauvajol, *Eur. Phys. J. B* 10, 263 (1999).

⁸ It is quite unlikely that the average tube diameter and/or the tube-tube spacing would be affected by annealing at 800 °C.

⁹ L. Henrard, A. Loiseau, C. Journet, and P. Bernier, *Eur. Phys. J. B* 13, 661 (2000).

¹⁰ Z. Benes, G. B. Vaughan, and J. E. Fischer (unpublished).

¹¹ J. Hone, M. C. Llaguno, N. M. Nemes, A. T. Johnson, J. E. Fischer, D. A. Walters, M. J. Casavant, J. Schmidt, and R. E. Smalley, *Appl. Phys. Lett.* 77, 666 (2000).